Neutron scattering study of soft optical phonons in $La_{2-x}Sr_xCuO_{4-y}$

T. R. Thurston, R. J. Birgeneau, D. R. Gabbe, H. P. Jenssen, M. A. Kastner, P. J. Picone,* and N. W. Preyer
Center for Materials Science and Engineering, Massachusetts Institute of Technology, Cambridge, Massachusetts 02139

J. D. Axe, P. Böni,† and G. Shirane
Brookhaven National Laboratory, Upton, New York 11973

M. Sato, K. Fukuda, and S. Shamoto
Institute for Molecular Science, Myodaiji, Okazaki 444, Japan
(Received 31 October 1988)

The soft optical phonons associated with the tetragonal-to-orthorhombic structural phase transition in $La_{2-x}Sr_xCuO_{4-y}$ have been investigated using inelastic-neutron-scattering techniques. Single crystals with Sr concentrations of $x=0$, 0.08, and 0.14 were studied. Both branches of the doubly degenerate X-point phonon which go soft at the tetragonal-to-orthorhombic transition have been observed in the orthorhombic phase. In all three samples one branch hardens, while the other remains relatively soft with behavior indicative of a further incipient structural phase transition. We identify the hard and soft branches of the orthorhombic phase as zone-center and zone-boundary phonons, respectively. The zone-center mode has A_g symmetry and is, consequently, Raman active. The relation of these measurements to other structural properties and to the superconductivity in $La_{2-x}Sr_xCuO_{4-y}$ is discussed.

I. INTRODUCTION

The $La_{2-x}R_xCuO_{4-y}$ class of high-T_c superconductors has been found to exhibit an unusually rich variety of phenomena in its transport, magnetic, and structural properties. This paper reports the results of inelastic-neutron-scattering studies on one aspect of the structural properties,[1] the soft optical phonons at the tetragonal X point in $La_{2-x}Sr_xCuO_{4-y}$. The X-point mode was first reported to go soft at the tetragonal-to-orthorhombic structural phase transition in Ref. 2, and subsequent measurements of the critical behavior associated with the tetragonal-to-orthorhombic transition are found in Ref. 3. In this report the focus will be on the behavior of the X-point phonons in the low-temperature orthorhombic phase and their relation to low-temperature structural phase transitions and anomalies. Raman scattering studies of some aspects of these soft optical phonons are reported in Refs. 4, 5, and 6.

Many recent powder-diffraction experiments have indicated that low-temperature structural instabilities exist in the orthorhombic phase of $La_{2-x}R_xCuO_{4-y}$. Experiments[7-9] on $La_{2-x}Ba_xCuO_{4-y}$ have reported actual transitions out of the orthorhombic phase in the 40–70 K temperature range. The new phase can be either tetragonal[7] or possibly monoclinic,[9] depending on the Ba concentration. Oxygen concentration may also play a critical but currently uncharacterized role in determining the low-temperature transition characteristics. Indeed, variations in oxygen concentration change the orthorhombic to tetragonal structural phase-transition temperature T_0 in La_2CuO_{4-y} quite drastically,[10,11] so changes with oxygen content in low-temperature structural transitions would not be surprising. In La_2CuO_{4-y} and $La_{2-x}Sr_xCuO_{4-y}$ most studies[12] have not reported transitions out of the *Cmca* phase. One exception in $La_{1.85}Sr_{0.15}CuO_4$ has been reported;[13] in this case the transition was at low temperatures ($T<30$ K). Again, variations in oxygen concentration may lead to different laboratories reporting different structural properties. We note that none of the samples in this study has low-temperature transitions out of the *Cmca* phase.

Measurements of the elastic properties have also indicated the presence of low-temperature structural instabilities.[14-18] All published results which we are aware of have been on polycrystalline samples, therefore, only information on bulk thermodynamic properties has been obtained. In both $La_{2-x}Ba_xCuO_{4-y}$ and $La_{2-x}Sr_xCuO_{4-y}$ the average velocity of the acoustic modes softens greatly (up to 40%) (Ref. 16) near T_0 (we denote the superconducting and high-temperature tetragonal-to-orthorhombic structural transitions by T_c and T_0, respectively). This change in elastic properties is undoubtedly related to the tetragonal-to-orthorhombic transition at T_0. In fact, coupling between the order parameter and strains can account for this softening quite naturally.[19] However, the acoustic modes remain soft for an extended temperature range below T_0, a fact suggesting that the *Cmca* phase is unstable. Further, in some barium-doped samples[18] a hardening at low temperatures suggestive of the low-temperature structural phase transition is seen.

We mention finally that various indirect measurements have corroborated the presence of structural anomalies and low-temperature transitions. In Ref. 8 the low-temperature transition directly observed in $La_{1.85}Ba_{0.15}CuO_4$ by neutron diffraction was accompanied by an anomaly in the resistance of the sample. Similar resistance anomalies have been seen[20] in Ba-doped samples with compositions in the range $0.10 \le x \le 0.125$, and subsequent diffraction work[21] has confirmed that a transition out of the *Cmca* phase does in fact occur in this range of Ba doping. Last, Raman scattering measurements[4] of the zone-center phonons have suggested the presence of phases other than the *Cmca* phase in Sr-doped samples; extra peaks are observed in the phonon Raman scattering whose presence is most easily explained if the samples have monoclinic symmetry.

The format of this paper is as follows. In Sec. II the crystal structure of La_2CuO_4 is discussed; we also describe the materials, transport, and magnetic properties of the samples studied. Our neutron-diffraction results are presented in Sec. III, and in Sec. IV we discuss our results and their relationship to the low-temperature structural transitions described above. Finally, in Sec. V we mention the possible connections of our results to the superconductivity in $La_{2-x}R_xCuO_{4-y}$.

II. PRELIMINARY DETAILS

The crystal structure of La_2CuO_4 is shown in Fig. 1(a). In the tetragonal phase the space group is $I4/mmm$ and in the orthorhombic phase it is *Cmca*;[22] the tetragonal-to-orthorhombic phase transition corresponds qualitatively to the rotation of CuO_6 octahedra shown. A map of the reciprocal lattice measured in orthorhombic units is shown in Fig. 1(b). Since the orthorhombic cell that is used for indexing the peaks is twice as big as the primitive *Cmca* cell, not every orthorhombic reciprocal-lattice Bragg position is a *Cmca* Bragg position. In the experiments presented here, most of the measurements were performed around the (0,2,3) superlattice peak, but because of twinning phonons around the (3,2,0) position were simultaneously measured. From Fig. 1(b) one can see that the (3,2,0) phonons have wave vectors at a boundary of the *Cmca* Brillouin zone. These phonons are consequently *not* Raman active; this is an important difference between our measurements and Raman studies.[4–6]

The single crystals used in this study were grown at the Institute for Molecular Science (IMS) and the Massachusetts Institute of Technology (MIT) by a CuO flux technique. Details of this growth technique are given in Refs. 23 and 24. Strontium and oxygen compositions and gradients may be estimated from measurements of the order parameter associated with the tetragonal-to-orthorhombic transition. Figure 2 shows data for a superlattice peak intensity versus temperature for the three samples. The Sr content of each doped sample was then estimated from the value of T_0 using Fig. 3 of Ref. 25. Confirmation of the Sr content in the $x=0.08$ sample was provided by electron probe microanalysis (EPMA). The oxygen content of the pure sample may be estimated from the value of T_0 and Refs. 10 and 11 to be $y=0.02$; however, we do not know values for y in the Sr-doped samples. Estimates of strontium and oxygen concentration gradients in the samples may be calculated from the amount of rounding in the tetragonal-to-orthorhombic structural phase transition temperature. From Fig. 2 of this paper and Refs. 10, 11, and 25 we estimate the variation in strontium and oxygen concentration to be less than 0.02 in all three samples. In calculating the oxygen concentration gradient, we assumed that the temperature dependence of T_0 on oxygen concentration in undoped La_2CuO_{4-y} is comparable to that in doped $La_{2-x}Sr_xCuO_{4-y}$. The estimates were therefore calculated in a conservative manner; we assumed that variation in only strontium or oxygen alone caused *all* of the rounding shown in Fig. 2.

A summary of physical properties of the samples studied is given in Table I. The undoped sample is an insulator which undergoes a three-dimensional (3D) antiferromagnetic phase transition at $T_N=240$ K. The $x=0.08$ sample undergoes a superconducting transition; the mid-

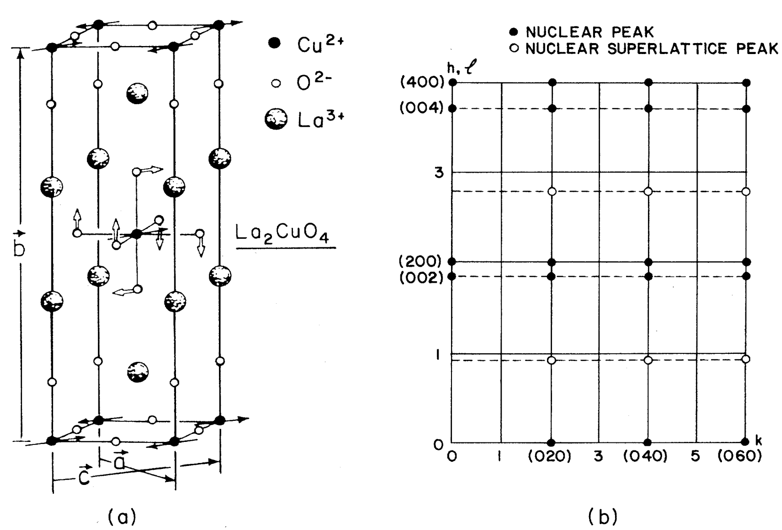

FIG. 1. (a) Crystal structure of La_2CuO_4; the arrows associated with the center oxygen indicate the direction of rotation in the orthorhombic phase. (b) Orthorhombic $(h,k,0)$ and $(0,k,l)$ reciprocal-lattice zones. The filled and open circles denote $I4/mmm$ nuclear peaks and *Cmca* nuclear superlattice peaks, respectively. Note that measurements at the (0,2,3) *Cmca* superlattice peak position also measure the (3,2,0) zone-boundary position because of twinning in the *Cmca* phase.

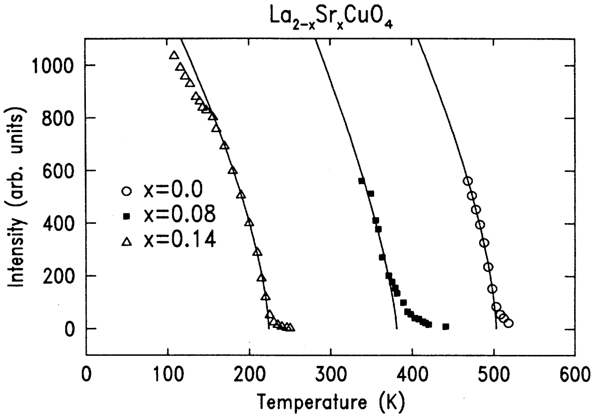

FIG. 2. Superlattice peak intensities in $La_{2-x}Sr_xCuO_{4-y}$. The solid lines represent the power law $I=I_0(T_0-T)^{2\beta}$. Values of β for the lines shown are 0.33, 0.37, and 0.34 for $x=0$, 0.08, and 0.14, respectively. The data is not sufficiently accurate to warrant interpretation of the values for β in terms of critical exponents, however.

point of the transition as measured by the resistivity was at ≈ 12 K, and the resistivity was zero at 4.2 K. Susceptibility measurements on a piece from the edge of the $x=0.08$ sample indicate a Meissner fraction of 15% at 5 K. Indications of a rather broad superconducting transition in the $x=0.14$ sample were also observed; the resistivity began to drop at ≈ 25 K, but the sample still had a finite resistance at the lowest temperature measured (2.5 K). In both Sr-doped samples no 3D antiferromagnetic transition occurs. The magnetic behavior of heavily doped samples is quite complicated; see Refs. 25 and 26 for more details.

III. NEUTRON SCATTERING MEASUREMENTS

Experiments were conducted on the triple-axis spectrometers H7 and H4M at the Brookhaven High Flux Beam Reactor. The detected neutron final energy was fixed at $E_f=14.7$ meV and different combinations of 20′ and 40′ collimators were used depending on the conflicting requirements of intensity and resolution. Neutrons with subharmonic wavelengths were removed by a pyrolytic graphite filter mounted after the analyzer crystal. Most measurements were performed in the orthorhombic $(h,k,0)$ and $(0,k,l)$ reciprocal-lattice zones shown in Fig. 1(b).

The soft X-point phonons may in principle be measured in the vicinity of any superlattice peak position; the position chosen for this study because of its favorable intensity was the orthorhombic (0,2,3). Typical triple-axis energy scans with peaks from inelastic phonon scattering are shown in Figs. 3 and 4. The scans were corrected for small residual higher-order neutron contamination[27] and then fit to the damped harmonic-oscillator cross section

$$S(\mathbf{q},E)=\frac{I_{\rm ph}}{1-\exp(-\beta E)}\left[\frac{\Gamma}{(E^2-E_{\rm ph}^2)^2+\Gamma^2E^2}+\frac{\Gamma}{(E^2+E_{\rm ph}^2)^2+\Gamma^2E^2}\right]\frac{1}{E}+I_G\exp(-E^2/2\sigma^2) \qquad (1)$$

convolved with the instrumental resolution function. In this cross section, β is $1/k_BT$, E is the energy transfer of the neutron, $E_{\rm ph}$ is the phonon energy, and Γ is a phenomenological damping constant. The Gaussian is included to fit the overdamped "central peak"[19] $(T>T_0)$ or superlattice peak $(T<T_0)$. In the fits, we have assumed $E_{\rm ph}$ to be constant within the instrumental resolution function, that is, we did not take into account the dispersion of the phonons.

Figure 5 shows the temperature dependence of the X-point phonon energy. Most of these phonon energies were measured at the (0,2,3.075) position instead of the (0,2,3) position because the soft phonons at the (0,2,3) position became so heavily overdamped that we could not resolve them from the superlattice peak $(T<T_0)$ or central peak $(T>T_0)$. Indeed, within 30 K of T_0 even the (0,2,3.075) phonon became impossible to resolve (see the $T=493$ K scan of Fig. 3). The dispersion of the phonons along the three orthorhombic reciprocal-lattice directions for the lower energy branch of the $x=0$ sample is shown in Fig. 6. The motivation for plotting the phonon energy squared against the phonon wave vector squared is discussed below.

Both the (0,2,3) zone-center mode *and* the (3,2,0) zone-boundary mode can be seen for temperatures below T_0 in Fig. 5. In order to identify the symmetry and wave vector of the two branches, we note that Raman scattering measurements[4–6] of the condensed zone-center mode in undoped La_2CuO_{4-y} coincide with the upper branch in Fig. 5(a). The measurements also identify the symmetry

TABLE I. Crystal properties.

Label	x	Volume (cm^3)	a (Å)[a]	b (Å)	c (Å)	T_0 (K)	T_N (K)	T_c (K)
MIT-10	0	1.6	5.359	13.152	5.405	503	240	···
IMS-1	0.08	1.6	5.364	13.189	5.364	381	···	≈ 12
MIT-13	0.14	1.0	5.357	13.221	5.357	224	···	···

[a] Lattice constants measured at 295 K.

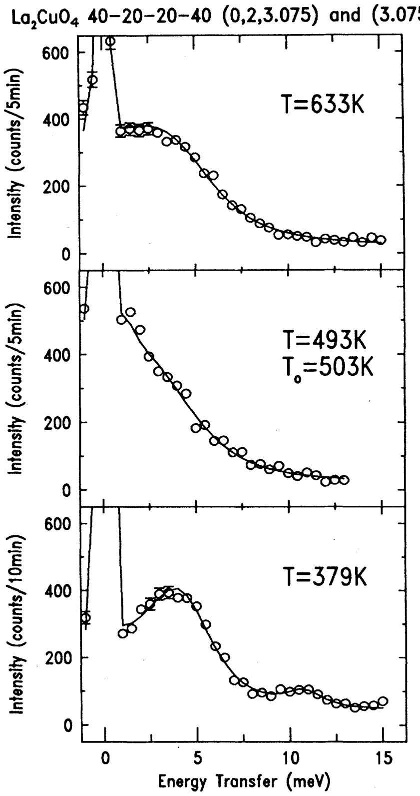

FIG. 3. Energy scans showing phonon peaks in the undoped sample. At 633 K the two X-point modes are degenerate, so only one peak is present. At 493 K, the two modes are not degenerate, but their energies are so close and their linewidths so large from overdamping that they cannot be resolved. At 379 K two distinct peaks from both the condensed zone-center mode and the uncondensed zone-boundary mode can be seen.

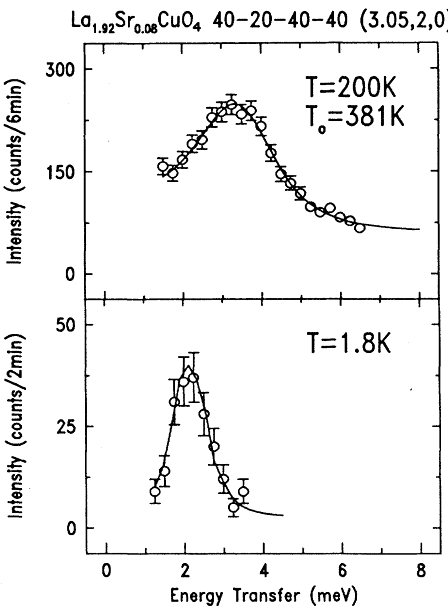

FIG. 4. Energy scans showing phonon peaks in the $x=0.08$ sample. Note the decrease in energy with decreasing temperature.

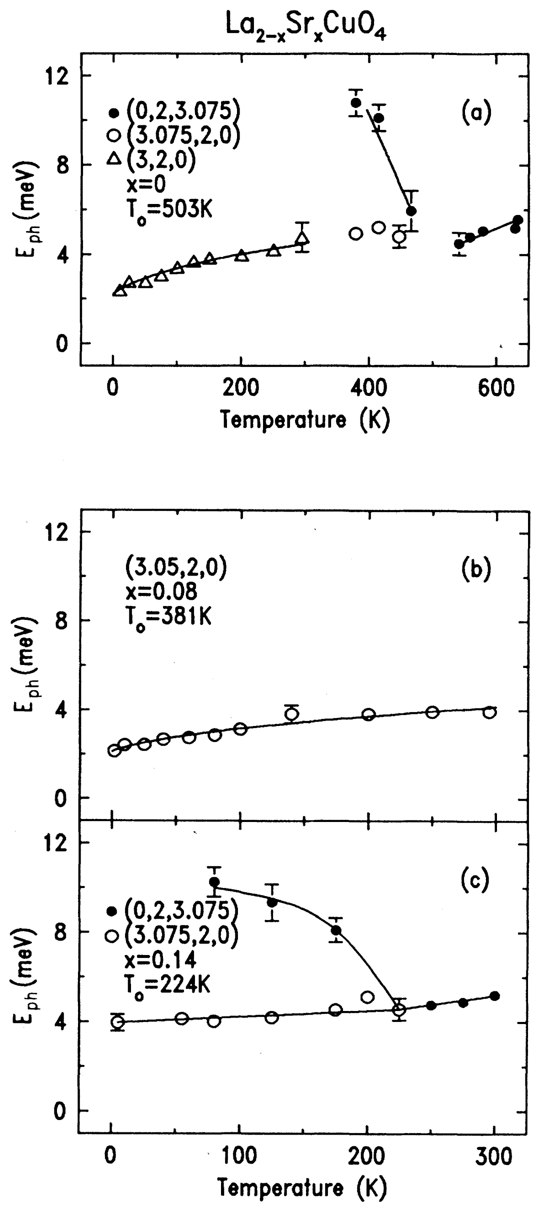

FIG. 5. Summary of the soft phonon energies in all three samples studied. The lines are guides to the eye.

of the condensed mode as A_g, as expected since the condensed mode must have the full symmetry of the low-temperature phase. The lower branch in Fig. 5(a) is then the uncondensed mode which is a zone-boundary mode with wave vector (3,2,0). We deduce from compatibility relations that the zone-boundary mode has Z_2^+ symmetry in the notation of Ref. 28.

Finally, we looked for differences in the soft (3,2,0) phonon in the superconducting and normal states. We observed no changes in the energy or linewidth of this phonon in the $x=0.08$ and $x=0.14$ samples studied here. Cursory measurements[29] performed on a $T_c=10$ K 80% Meissner $La_{1.89}Sr_{0.11}CuO_4$ sample also revealed no differences in the normal and superconducting states.

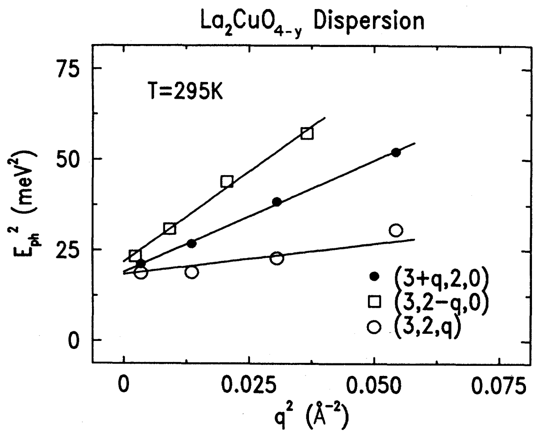

FIG. 6. Dispersion of the soft mode branch along the orthorhombic (0,1,0), (1,0,0), and (0,0,1) directions.

IV. DISCUSSION

We shall discuss most of our results within the context of Landau theory.[3,7] The order parameter of this system has two components (Q_α, Q_β) corresponding to the two X-point soft phonons with wave vectors at $(\frac{1}{2},\frac{1}{2},0)$ and $(\frac{1}{2},\bar{\frac{1}{2}},0)$ (tetragonal units); the free energy of the system is then

$$G=\tfrac{1}{2}a(T-T_0)(Q_\alpha^2+Q_\beta^2)+u(Q_\alpha^2+Q_\beta^2)^2+v(Q_\alpha^4+Q_\beta^4)+\cdots \quad (2)$$

Here a, u, and v are weakly temperature-dependent constants. The symmetry of this free energy puts this system in the 3D XY with cubic anisotropy universality class; we mention in passing that a renormalization-group analysis of this model has been done by Aharony.[30,31] Further, the order-parameter data shown in Fig. 2, while not sufficiently accurate to warrant interpretation in terms of critical exponents, is consistent with both theory[30,31] and previous experiments.[3]

The soft-mode energy squared is proportional to the inverse susceptibility $\partial^2G/\partial Q^2$. Using the Landau free energy G given above with fluctuations included in lowest order gives for the soft-mode energy squared,

$$E_{\mathrm{ph}}^2=a(T-T_0)+\mathbf{q}\cdot\mathbf{B}\cdot\mathbf{q}\,, \quad (3a)$$

$$E_{\mathrm{ph}}^2=2a(T_0-T)+\mathbf{q}\cdot\mathbf{B}\cdot\mathbf{q}\,, \quad (3b)$$

$$E_{\mathrm{ph}}^2=-\frac{av}{u+v}(T_0-T)+\mathbf{q}\cdot\mathbf{B}\cdot\mathbf{q}\,. \quad (3c)$$

Equation (3a) applies above T_0, while (3b) and (3c) correspond to the condensed and uncondensed modes respectively below T_0. In our analysis, we have assumed that $Q_\beta=0$ in the *Cmca* phase, and also have let $\mathbf{q}\cdot\mathbf{B}\cdot\mathbf{q}=b_1q_1^2+b_2q_2^2+b_3q_3^2$ where the q_i are measured along orthorhombic axes. We note that this form of the dispersion is consistent with the symmetry of the system. The slopes of the lines shown in Fig. 6 give dispersion constants of $b_2=1130$, $b_1=620$, and $b_3=250$ meV Å^2 at 295 K in the $x=0$ sample; we observed only moderate dependencies on the temperature and Sr concentration for these constants. Given the lamellar nature of the material one may have expected that the $(0,k,0)$ orthorhombic direction would be nearly dispersionless. Our measurements show that this is not the case. Indeed, simple calculations of the lattice dynamics of near-neighbor-coupled rigid CuO_6 octahedra are in qualitative agreement with our measurements if strong interlayer coupling is invoked. The basically isotropic behavior of the phonon dispersion indicates that critical fluctuations associated with the tetragonal-to-orthorhombic transition will also be isotropic. This in turn means that the critical behavior of this system is not that of a uniaxial Lifshitz point,[19,32] a model with anisotropic critical fluctuations which could have explained the relatively low values for β measured previously.[3]

We now discuss the low-temperature behavior of the uncondensed mode below T_0 shown in Figs. 5(a)–5(c). The most important features of this mode are its relatively low energy and the softening at low temperatures. The low energy of this mode suggests that the orthorhombic phase of $La_{2-x}Sr_xCuO_{4-y}$ is inherently unstable. Within Landau theory, minimization of Eq. (2) reveals that only two stable phases can exist.[7,19]

(1) A phase where one of the Q_i is zero and the other nonzero. This corresponds to the orthorhombic phase and will occur when $v<0$ and $v+u>0$.

(2) A phase where $|Q_\beta|=|Q_\alpha|$. This corresponds to a tetragonal phase and will occur when $v>0$ and $2u+v>0$. Such a transition has in fact been observed in $La_{2-x}Ba_xCuO_{4-y}$,[7] and La_2CoO_4.[33]

Since $v<0$ in the *Cmca* phase, while $v>0$ in a low-temperature tetragonal phase, any transformation between these two phases occurs when the Landau parameter $v\rightarrow 0$. The temperature dependence of v in the orthorhombic phase may be calculated in Landau theory to be

$$v=-\frac{E_{\mathrm{ph}}^2}{4Q_\alpha^2}\,. \quad (4)$$

Here E_{ph} refers to the uncondensed zone-boundary mode of the *Cmca* phase. We have used the data for E_{ph} of Fig 5(a) and the data for Q_α of Ref. 34 to calculate the temperature dependence of v; Fig. 7 shows the results of this

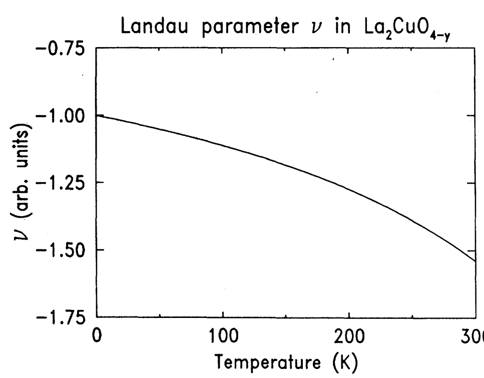

FIG. 7. Landau parameter v for the $(Q_\alpha^4+Q_\beta^4)$ term in Eq. (2). The decrease of v at low temperatures is indicative of an incipient structural phase transition.

calculation. The softening of v as $T \rightarrow 0$ indicates that La_2CuO_{4-y} has an incipient structural phase transition similar to those actually present in $La_{2-x}Ba_xCuO_{4-y}$ and La_2CoO_4.

V. STRUCTURAL INSTABILITIES AND SUPERCONDUCTIVITY

The incipient structural instability of the *Cmca* orthorhombic phase manifested by the soft zone-boundary mode is almost certainly not a primary mechanism for the high-temperature superconductivity in $La_{2-x}Sr_xCuO_{4-y}$. Nonetheless, structural effects may still play a secondary role in the superconductivity. We cite two experimental observations which reinforce this line of thought. (1) The isotope effect measured in $La_{2-x}R_xCuO_{4-y}$ is not negligible.[35,36] (2) A strong correlation between measured values of T_c and low-temperature structural phase transitions in the $La_{2-x}Ba_xCuO_4$ system has been reported by Moodenbaugh and co-workers[20] and Axe and Moudden.[21] Recent calculations[37] have also indicated that the rotational X-point modes responsible for the tetragonal-to-orthorhombic transition do couple to electron states at the Fermi level. Clearly the relationship of structural instabilities to the superconductivity in $La_{2-x}R_xCuO_{4-y}$ is not completely understood yet; more measurements on Ba-doped samples in particular and further calculations of the electron-phonon coupling are needed to resolve this issue.

ACKNOWLEDGMENTS

We acknowledge useful discussions with A. Aharony and J. O. Fossum. This work is supported by the U.S.-Japan Cooperative Neutron Scattering Program, and a Grant-in-Aid for Scientific Research from the Japanese Ministry of Education, Science, and Culture. The work at MIT is supported by the National Science Foundation under Contracts No. DMR 85-01856 and No. DMR 84-18718. Research at Brookhaven is supported by the Division of Materials Sciences, U.S. Department of Energy under Contract No. DE-AC02-76CH00016.

---

*Permanent address: Defense Science Technology Organization, Adelaide, Australia.

†Permanent address: Paul Scherrer Institut, 5303 Würenlingen, Switzerland.

[1] J. D. Jorgensen, in *Proceedings of the Eighteenth International Conference on Low Temperature Physics* [Jpn. J. Appl. Phys. Suppl. 3 **26**, 2017 (1987)].

[2] R. J. Birgeneau, C. Y. Chen, D. R. Gabbe, H. P. Jenssen, M. A. Kastner, C. J. Peters, P. J. Picone, T. Thio, T. R. Thurston, H. L. Tuller, J. D. Axe, P. Böni, and G. Shirane, Phys. Rev. Lett. **59**, 1329 (1987).

[3] P. Böni, J. D. Axe, G. Shirane, R. J. Birgeneau, D. R. Gabbe, H. P. Jenssen, M. A. Kastner, C. J. Peters, P. J. Picone, and T. R. Thurston, Phys. Rev. B **38**, 185 (1988).

[4] S. Sugai, this issue, Phys. Rev. B **39**, 4036 (1989).

[5] W. H. Weber, C. R. Peters, B. M. Wanklyn, Changkang Chen, and B. E. Watts, Solid State Commun. **68**, 61 (1988).

[6] G. Burns, G. V. Chandrashekhar, F. H. Dacol, and M. W. Shafer, Solid State Commun. **68**, 67 (1988).

[7] J. D. Axe, D. E. Cox, K. Mohanty, A. Moodenbaugh, H. Moudden, Y. Xu, and T. R. Thurston, IBM J. Res. Dev. (to be published).

[8] D. Mck. Paul, G. Balakrishnan, N. R. Beinhoeft, W. I. F. David, and W. T. A. Harrison, Phys. Rev. Lett. **58**, 1976 (1987).

[9] S. C. Moss, K. Forster, J. D. Axe, H. You, D. Hohlwein, D. E. Cox, P. H. Hor, R. L. Meng, and C. W. Chu, Phys. Rev. B **35**, 7195 (1987).

[10] D. C. Johnston, J. P. Stokes, D. P. Goshorn, and J. T. Lewandowski, Phys. Rev. B **36**, 4007 (1987).

[11] D. C. Johnston, S. K. Sinha, A. J. Jacobson, and J. M. Newsam, Physica C **153–155**, 572 (1988).

[12] R. M. Fleming, B. Batlogg, R. J. Cava, and E. A. Rietman, Phys. Rev. B **35**, 7191 (1987); R. Moret, J. P. Pouget, and G. Collin, Europhys. Lett. **4**, 365 (1987); J. O. Fossum and W. Fu (unpublished).

[13] P. Day, M. Rosseinsky, K. Prassides, W. I. F. David, O. Moze, and A. Soper, J. Phys. C **20**, L429 (1987).

[14] S. Bhattacharya, M. J. Higgins, D. C. Johnston, A. J. Jacobson, J. P. Stokes, D. P. Goshorn, and J. T. Lewandowski, Phys. Rev. Lett. **60**, 1181 (1988).

[15] Y. Horie, Y. Terashi, H. Fukuda, T. Fukami, and S. Mase, Solid State Commun. **64**, 501 (1987).

[16] X. D. Xiang, J. W. Brill, L. E. Delong, L. C. Bourne, A. Zettl, J. C. Jones, and L. A. Rice, Solid State Commun. **65**, 1073 (1988).

[17] P. Esquinazi, J. Luzuriaga, C. Duran, D. A. Esparza, and C. O'Ovidio, Phys. Rev. B **36**, 2316 (1987).

[18] K. Fossheim, T. Laegreid, E. Sandvold, F. Vassenden, K. A. Müller, and J. G. Bednorz, Solid State Commun. **63**, 531 (1988).

[19] A. D. Bruce and R. A. Cowley, *Structural Phase Transitions* (Taylor and Francis LTD, London, 1981).

[20] A. R. Moodenbaugh, Y. Xu, and M. Suenega, Proc. Mater. Res. Soc. **99**, 427 (1987); A. R. Moodenbaugh, Youwen Xu, M. Suenaga, T. J. Folkerts and R. N. Shelton, Phys. Rev. B **38**, 4596 (1988).

[21] J. D. Axe and H. Moudden (unpublished).

[22] J. D. Jorgensen, H. B. Schüttler, D. G. Hinks, D. W. Capone II, K. Zhang, M. B. Brodsky, and D. J. Scalapino, Phys. Rev. Lett. **58**, 1024 (1987).

[23] S. Shamoto, S. Hosoya, and M. Sato, Solid State Commun. **66**, 195 (1988).

[24] P. J. Picone, H. P. Jenssen, and D. R. Gabbe, J. Cryst. Growth **85**, 576 (1987).

[25] R. J. Birgeneau, D. R. Gabbe, H. P. Jenssen, M. A. Kastner, P. J. Picone, T. R. Thurston, G. Shirane, Y. Endoh, M. Sato, K. Yamada, Y. Hidaka, M. Oda, Y. Enomoto, M. Suzuki, and T. Murakami, Phys. Rev. B **38**, 6614 (1988).

[26] R. J. Birgeneau, Y. Endoh, Y. Hidaka, K. Kakurai, M. A. Kastner, T. Murakami, G. Shirane, T. R. Thurston, and K. Yamada, Phys. Rev. B **39**, 2868 (1989).

[27] R. A. Cowley, G. Shirane, R. J. Birgeneau, and H. J. Guggenhiem, Phys. Rev. B **15**, 4292 (1977).

[28] J. C. Slater, G. F. Koster, and J. H. Wood, Phys. Rev. **126**, 1307 (1962).

[29] T. R. Thurston (private communication).

[30]A. Aharony, Phys. Rev. B **8**, 4270 (1973).
[31]A. Aharony, in *Phase Transitions and Critical Phenomena,* edited by C. Domb and M. S. Green (Academic, New York, 1976), Vol. 6, p. 357.
[32]A. Aharony and A. D. Bruce, Phys. Rev. Lett. **42**, 462 (1979).
[33]K. Yamada, M. Matsuda, Y. Endoh, B. Keimer, R. J. Birgeneau, S. Onodera, J. Mizusaki, T. Matsuura, and G. Shirane, Phys. Rev. B **39**, 2336 (1989).
[34]D. Vaknin, S. K. Sinha, D. E. Moncton, D. C. Johnston, J. M. Newsam, C. R. Safinya, and H. E. King, Jr., Phys. Rev. Lett. **58**, 2802 (1987).
[35]B. Batlogg, G. Kourouklis, W. Weber, R. J. Cava, A. Jayaraman, A. E. White, K. T. Short, L. W. Rupp, and E. A. Rietman, Phys. Rev. Lett. **59**, 912 (1987).
[36]T. A. Faltens, W. K. Ham, S. W. Keller, K. J. Leary, J. N. Michaels, A. M. Stacy, H. Loye, D. E. Morris, T. W. Barbee, L. C. Bourne, M. L. Cohen, S. Hoen, and A. Zettl, Phys. Rev. Lett. **59**, 915 (1987).
[37]R. E. Cohen, W. E. Pickett, and H. Krakauer (unpublished).